# A VIRTUAL ELEMENT APPROACH FOR MICROPOLAR CONTINUA

**M. PINGARO*, M. L. DE BELLIS† AND P. TROVALUSCI***

* Department of Structural and Geotechnical Engineering
Sapienza University of Rome
Via Gramsci 53, 00197 Rome, Italy
e-mail: marco.pingaro@uniroma1.it, patrizia.trovalusci@uniroma1.it - Web page: http://www.uniroma1.it

† Department of Engineering and Geology
Gabriele dAnnunzio University
Viale Pindaro 42, 65122 Pescara, Italy
e-mail: marialaura.debellis@unich.it - Web page: http://www.unich.it

**Key words:** Cosserat Continua, Virtual Element Method (VEM)

**Abstract.** In this work we propose a novel virtual element approach for solving boundary value problems in 2D linear isotropic micropolar elasticity. Following the basic idea of the Virtual Element Method (VEM), the degrees of freedom of each material point, i.e. the displacement and rotation fields, are decomposed into both a polynomial space, either linear or quadratic, and a remaining space that is kept virtual in the formulation. Generalized consistency and stabilization terms are consistently derived.
Different patch tests, properly conceived for micropolar continua, are proposed and compared to reference solutions present in literature. The obtained results are in good agreement with these solutions, confirming the capability of the proposed elements in the modelling of the expected responses.
The expected applications of this methodology concern the mechanical study of microstructured materials, inherently characterized by nonlocal response, which has been widely proven to be effectively represented by micropolar continua.

## 1 INTRODUCTION

A wide range of microstructured materials, commonly adopted in different engineering applications, is strongly characterized by nonlocal response, due to the presence of internal lengths and related dispersion properties [37, 32, 30]. This behaviour is especially evident for materials with characteristic sizes at the microstructure that are comparable to a structural length. Examples include fiber-beam networks, polycristals, foams, cancellous bones, but also metal matrix composites or masonry-like materials [34, 29, 19]. In all such cases, the overall constitutive behaviour is influenced by scale parameters, directly

related to the dimension of heterogeneities, that are typically non negligible with respect to the characteristic structural size.
In this context, the micropolar continuum, that belongs to the class of generalized continua [11], is able to retain memory of an inherent microstructure, providing an enriched constitutive behaviour, with respect to the classical Cauchy continuum. Each material point is, indeed, provided with displacement and rotation degrees of freedom, thus resulting in additional strains and stresses: besides the classical components, micropolar ones include curvatures (work conjugate to couple stresses) and skew-symmetric strains (work conjugate to skew-symmetric stresses).
From the experimental point of view, micropolar effects have been captured and identified in several materials ranging from natural materials [17, 28, 27, 18], up to engineered materials obtained via 3D printing techniques [26]. On the other hand, from the numerical modelling point of view different approaches have been proposed including micromechanical modelling [24, 13, 1, 4, 12, 19] and multi-scale modelling [31, 35, 16, 33, 21, 15, 36]. In most cases finite element analyses have been performed in order to solve boundary value problems at different scales of interest [12, 19]. As an alternative to the Finite element method, the Virtual Element Method (VEM) has been recently proposed [5, 6], representing an extension of mimetic finite difference approaches to deal with very general polygonal elements with generic number of nodes. The VEM is proving to be a very effective numerical tool, characterized by high flexibility especially concerning the modelling of very complex geometries, hanging nodes and very robust with respect to mesh distortion. Many applications have been presented so far ranging from linear elasticity [23, 22, 25, 8, 20] up to non-linear problems [10, 2, 3, 14].
In this work, we propose a virtual element approach for solving boundary value problems in 2D linear isotropic micropolar elasticity. Following the basic idea of the method, here, the displacement and rotation fields are decomposed into a polynomial space, either linear or quadratic, and a remaining space that is kept virtual in the formulation. Generalized consistency and stabilization terms are consistently derived.
Different applications are proposed [24], ranging from a patch test, properly conceived for micropolar continua, to various engineering applications. The obtained results are in good agreement with reference solutions, confirming the capability of the proposed elements in modelling the expected responses.

## 2 VIRTUAL FORMULATION FOR COSSERAT MEDIA

In this section we recall the governing equations of 2D linear elastic Cosserat continuum adopted in the presented study and describe the related virtual element space [5, 6], as well as the construction of the bilinear forms resulting from the weak form.
We consider a two–dimensional domain in the space $\mathbf{R}^2$, where the Cartesian coordinate system $(O, x, y)$ is introduced. The body is subjected to the volume force, represented by the vector $\boldsymbol{f} \in (L^2(\Omega))^2$, $\boldsymbol{f} = \{f_1, f_2\}^T$, and body couple represented by the scalar $m \in L^2(\Omega)$, $m = m_3$, where $L^2(\Omega)$ is the standard Lebesgue space. For the sake of simplicity we use homogeneous Dirichlet boundary conditions and consider the Sobolev spaces, $Q := H_0^1(\Omega)$ and $\boldsymbol{V} := [Q]^2$. We introduce the admissible displacement fields

$\boldsymbol{v} \in \boldsymbol{V}$ and the admissible rotation fields $\varphi_3 \in Q$.

Under the hypothesis of small deformations, the kinematical descriptors are the displacement field vector $\boldsymbol{u} = \{u_1,\, u_2\}^T$ and the scalar rotation field $\omega = \omega_3$. The corresponding strain measures are the strain vector $\boldsymbol{\varepsilon} = \{\varepsilon_{11},\, \varepsilon_{22},\, \varepsilon_{12},\, \varepsilon_{21}\}^T$ and the curvature vector $\boldsymbol{\kappa} = \{\kappa_1,\, \kappa_2\}^T$. The compatibility equations write:

$$\begin{cases} \varepsilon_{ij} = u_{j,i} + e_{ji}\,\omega\,, \\ \kappa_j = \omega_{,j}\,, \end{cases} \tag{1}$$

where $e_{ij}$ is the two-dimensional permutation tensor. Whereas the equilibrium equations are:

$$\begin{cases} \sigma_{ij,i} + f_j = 0\,, \\ \mu_{i,i} + e_{jk}\,\sigma_{jk} + m = 0\,, \end{cases} \tag{2}$$

where $\boldsymbol{\sigma}$ is the non–symmetric stress vector $\boldsymbol{\sigma} = \{\sigma_{11},\, \sigma_{22},\, \sigma_{12},\, \sigma_{21}\}^T$ and $\boldsymbol{\mu}$and the and couple stress vector is $\boldsymbol{\mu} = \{\mu_1,\, \mu_2\}^T$.

In the case of 2D isotropic linear elasticity we adopt the following constitutive equations [24]

$$\begin{aligned} \sigma_{ij} &= \mathbb{A}_{ijhk}\,\varepsilon_{hk}\,, \\ \mu_i &= 4Gl^2\,\kappa_i\,, \end{aligned} \tag{3}$$

where the elastic tensor of the fourth order $\mathbb{A}$ is:

$$\mathbb{A} = G \begin{bmatrix} \frac{2(1-\nu)}{1-2\nu} & \frac{2\nu}{1-2\nu} & 0 & 0 \\ \frac{2\nu}{1-2\nu} & \frac{2(1-\nu)}{1-2\nu} & 0 & 0 \\ 0 & 0 & 1+k & 1-k \\ 0 & 0 & 1-k & 1+k \end{bmatrix}, \tag{4}$$

where $G$ is the shear modulus, $\nu$ is the Poisson modulus, and $l$ is the length scale material constant. $k = G_c/G$ is the ratio between the Cosserat shear modulus $G_c$ and the standard shear modulus $G$. The weak form of the linear elastic problem reads:

$$\begin{cases} \text{Find } (\boldsymbol{u}, \omega) \in \boldsymbol{V} \times Q \text{ such that :} \\ a(\boldsymbol{u}, \boldsymbol{v}) + b(\omega, \boldsymbol{v}) = <\boldsymbol{f}, \boldsymbol{v}> \quad \forall \boldsymbol{v} \in \boldsymbol{V} \\ b(\boldsymbol{u}, \varphi) + c(\omega, \varphi) = <m, \varphi> \quad \forall \varphi \in Q \end{cases} \tag{5}$$

where:

$$\begin{aligned} a(\boldsymbol{u}, \boldsymbol{v}) &= \int_\Omega \mathbb{A}_{ijhk}\, u_{h,k}\, v_{i,j}\, d\Omega\,, \\ b(\omega, \boldsymbol{v}) &= \int_\Omega \mathbb{A}_{ijhk}\, e_{hk}\, \omega\, v_{i,j}\, d\Omega\,, \\ c(\omega, \varphi) &= \int_\Omega \left(\mathbb{A}_{ijhk}\, e_{hk}\, e_{ij}\, \omega\, \varphi\right) + \left(2Gl^2\, \omega_{,n} \varphi_{,n}\right)\, d\Omega\,, \\ <\boldsymbol{f}, \boldsymbol{v}> &= \int_\Omega f_i\, v_i\, d\Omega\,, \\ <m, \varphi> &= \int_\Omega m\, \varphi\, d\Omega\,. \end{aligned} \tag{6}$$

In order to approximate the solution of the problem (5) we consider a decomposition $\mathcal{T}_h$ of the domain $\Omega$ into non overlapping polygonal elements $E$. In the following, we denote by $e$ the straight edges of the mesh $\mathcal{T}_h$ and, for all $e \in \partial E$, $\boldsymbol{n}_i$ denotes the outward unit normal vector to $e_i$. The symbol $n_e$ represents the number of the edges of the polygon $E$, that coincides with the number of the element vertices.

Let $k$ be an integer $\geq 1$. Let us denote by $P_k(\Omega)$ the space of polynomials, living on the set $\Omega \subseteq \mathbb{R}^2$, of degree less than or equal to $k$.

By the discretization introduced, it is possible to write the bilinear forms (5), as in the finite element methodology, in the following way:

$$\begin{aligned} a(\boldsymbol{u}, \boldsymbol{v}) &= \sum_{E \in \mathcal{T}_h} a^E(\boldsymbol{u}, \boldsymbol{v}) \quad \forall \boldsymbol{v} \in \boldsymbol{V} \,, \\ b(\omega, \boldsymbol{v}) &= \sum_{E \in \mathcal{T}_h} b^E(\omega, \boldsymbol{v}) \quad \forall \boldsymbol{v} \in \boldsymbol{V} \,, \\ c(\omega, \varphi) &= \sum_{E \in \mathcal{T}_h} c^E(\omega, \varphi) \quad \forall \varphi \in Q \,, \end{aligned} \tag{7}$$

The discrete virtual element spaces, $\boldsymbol{V}_h$ and $Q_h$, are:

$$\begin{aligned} \boldsymbol{V}_h &:= \left\{ \boldsymbol{v} \in \boldsymbol{V} \,:\, \boldsymbol{v} \,|_E \in \boldsymbol{V}_{h|E} \, \forall E \in \mathcal{T}_h \right\} \,, \\ Q_h &:= \left\{ q \in Q \,:\, q \,|_E \in \; Q_{h|E} \, \forall E \in \mathcal{T}_h \right\} \,, \end{aligned} \tag{8}$$

where $\boldsymbol{V}_{h|E} := \left(V_{h|E}\right)^2$ and the local spaces $V_{h|E}$ and $Q_{h|E}$ are defined as

$$\begin{aligned} V_{h|E} &:= \left\{ v_h \in H^1(E) \cap C^0(E) : \, \triangle v_h \in P_{k-2}(E), \; v_h \,|_e \in P_k(e) \, \forall e \in \partial E \right\} \,, \\ Q_{h|E} &:= \left\{ q_h \in H^1(E) \cap C^0(E) : \, \triangle q_h \in P_{k-2}(E), \; q_h \,|_e \in P_k(e) \, \forall e \in \partial E \right\} \,. \end{aligned} \tag{9}$$

By the definition of the local spaces (9), we can observe that, in contrast to the standard finite element approach, the local spaces, $\boldsymbol{V}_{h|E}$ and $Q_{h|E}$, are not fully explicit, in fact $\boldsymbol{V}_{h|E}$ and $Q_{h|E}$ contain all the polynomials of degree $\leq k$, plus other functions that, in general, will not be polynomials. Moreover $\boldsymbol{v}_h$ is a polynomial of degree $k$ on each edge $e$ of $E$ and globally continuous on $\partial E$.

The problem (5) restricted to the discrete spaces $\boldsymbol{V}_h$ and $Q_h$ becomes:

$$\begin{cases} \text{Find } (\boldsymbol{u}_h, \omega_h) \in \boldsymbol{V_h} \times Q_h \text{ such that} \\ a_h(\boldsymbol{u}_h, \boldsymbol{v}_h) + b(\omega_h, \boldsymbol{v}_h) = < \boldsymbol{f}, \boldsymbol{v}_h > \quad \forall \boldsymbol{v}_h \in \boldsymbol{V_h} \,, \\ b(\boldsymbol{u}_h, \varphi_h) + c(\omega_h, \varphi_h) = < m, \varphi_h > \quad \forall \varphi \in Q_h \,, \end{cases} \tag{10}$$

where $a_h(\cdot,\cdot) : \boldsymbol{V}_h \times \boldsymbol{V}_h \to \mathbb{R}$, $b_h(\cdot,\cdot) : \boldsymbol{V}_h \times Q_h \to \mathbb{R}$ and $c_h(\cdot,\cdot) : Q_h \times Q_h \to \mathbb{R}$ are the discrete bilinear forms approximating the continuous forms $a(\cdot,\cdot)$, $b(\cdot,\cdot)$ and $c(\cdot,\cdot)$ respectively. $< \boldsymbol{f}, \boldsymbol{v}_h >$ and $< m, \varphi_h >$ are the terms approximating the virtual work of external loads.

**Table 1**: Patch test: coordinates nodes

| Node | x | y |
|---|---|---|
| 1 | 0.04 | 0.02 |
| 2 | 0.18 | 0.03 |
| 3 | 0.16 | 0.08 |
| 4 | 0.08 | 0.08 |
| 5 | 0.00 | 0.00 |
| 6 | 0.24 | 0.00 |
| 7 | 0.24 | 0.12 |
| 8 | 0.00 | 0.12 |

The discrete bilinear forms are constructed element by element as:

$$\begin{aligned} a_h(\boldsymbol{u}_h, \boldsymbol{v}_h) &= \sum_{E \in \mathcal{T}_h} a_h^E(\boldsymbol{u}_h, \boldsymbol{v}_h) \quad \forall \boldsymbol{u}_h,\ \boldsymbol{v}_h \in \boldsymbol{V}_h\ , \\ b_h(\omega_h, \boldsymbol{v}_h) &= \sum_{E \in \mathcal{T}_h} b_h^E(\omega_h, \boldsymbol{v}_h) \quad \forall \omega_h \in Q_h,\ \ \forall \boldsymbol{v}_h \in \boldsymbol{V}_h\ , \\ c_h(\omega_h, \varphi_h) &= \sum_{E \in \mathcal{T}_h} c_h^E(\omega_h, \varphi_h) \quad \forall \omega_h,\ \varphi_h \in Q_h\ . \end{aligned} \tag{11}$$

The local stiffness matrices can be derived, consistently with [6, 9], after introducing the local $L^2$-projection operators $\boldsymbol{\Pi}_E^\nabla : \boldsymbol{V}_h(E) \to (\mathbb{P}_k(E))^2$, $\Pi_E^\nabla : Q_h(E) \to \mathbb{P}_k(E)$ and $\Pi_E^0 : Q_h(E) \to \mathbb{P}_k(E)$.

The details on the construction of the local stiffness matrix are presented in [6, 9, 7, 22], while are here omitted for the sake of brevity.

## 3 NUMERICAL RESULTS

In this section we report a patch test to prove the reliability and the performances of the developed VEM Cosserat element. The patch test presented has been proposed by [24] and it was specifically conceived for Cosserat finite elements.

We consider a rectangular region discretized using two type of mesh: the first type is made by non-overlapping distorted triangular elements, Fig. 1(a), while the second by Voronoi elements, Fig. 1(b). The coordinates of the nodes for the triangular mesh are reported in the Tab. 1. We impose different boundary conditions (three different cases are analysed in the following) and both strains and stresses are checked [24]. Satisfaction of the patch tests guarantees stability and convergence of the element's solution [38] when used for the solution of real problems. For all tests we set the elastic constants: $G = 1000$, $\nu = 0.25$, $l = 0.1$ and $k = 0.5$.

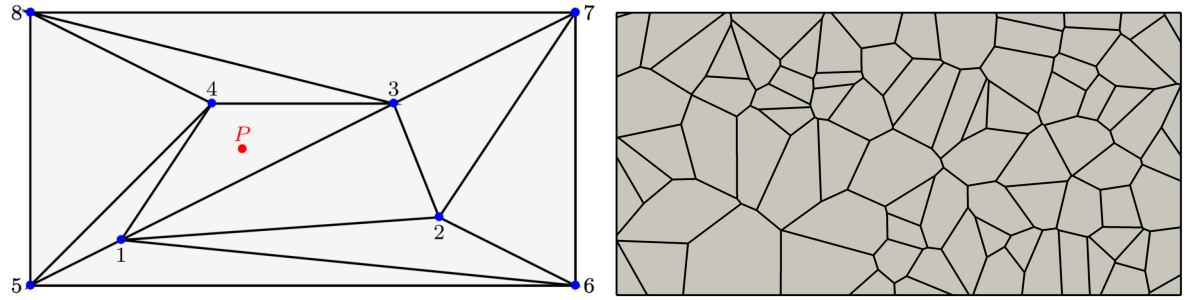


(a) Triangular element mesh (b) Voronoi mesh

**Figure 1**: Domain problem and the two relative mesh adopted

### 3.1 Patch Test 1

The first test is developed to check the capabilities of the element to reproduce the linear elastic Cauchy continuum. We impose the following boundary conditions in terms of displacements, $\boldsymbol{u}$, and rotation, $\omega$

$$\begin{aligned} u_1 &= 10^{-3}\left(x_1 + (1/2)x_2\right) \,, \\ u_2 &= 10^{-3}\left(x_1 + x_2\right) \,, \\ \omega &= (1/4)\,10^{-3} \,, \\ f_1 &= f_2 = 0 \,, \\ m &= 0 \,, \end{aligned} \tag{12}$$

and the relative analytical solution are:

$$\begin{aligned} \sigma_{11} &= \sigma_{22} = 4 \,, \\ \sigma_{12} &= \sigma_{21} = 1.5 \,, \\ \mu_1 &= \mu_2 = 0 \,. \end{aligned} \tag{13}$$

The stress, $\boldsymbol{\sigma}$, is constant and symmetric and the couple, $\boldsymbol{\mu}$, is identically null. In Fig. 2 we report the solution in terms of displacements for the two type of meshes adopted. In Figs. 3 and 4 the map color of the stresses for the two different mesh adopted are reported.

### 3.2 Patch Test 2

The following patch test was suited to check the capabilities to account for constant non-symmetric stress and identically null couple. We impose the following boundary

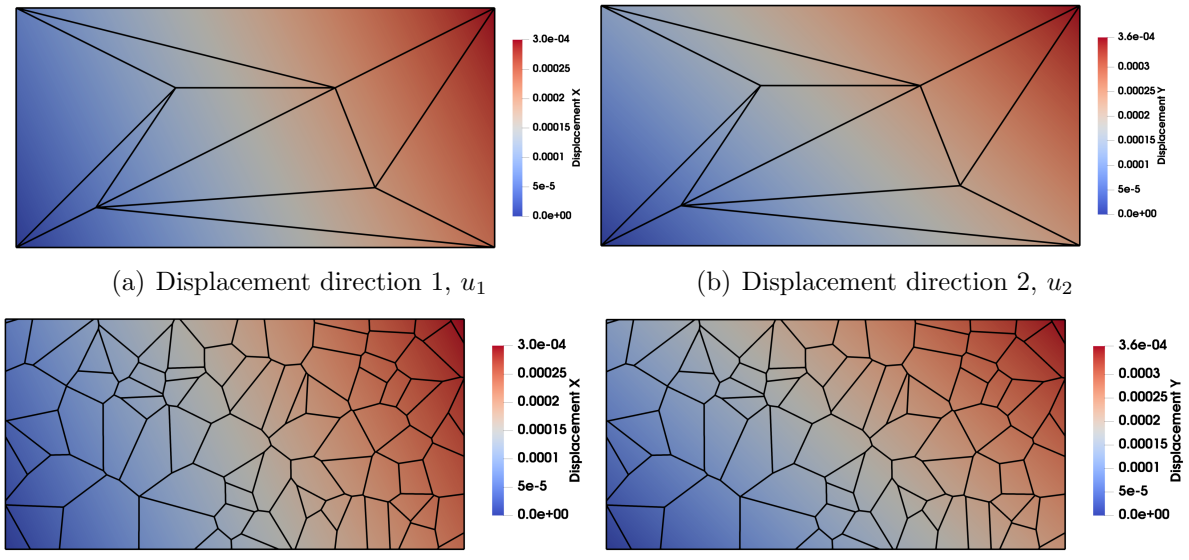


(a) Displacement direction 1, $u_1$

(b) Displacement direction 2, $u_2$

(c) Displacement direction 1, $u_1$

(d) Displacement direction 2, $u_2$

**Figure 2**: Displacement solution obtained for all tests with triangular and Voronoi meshes, respectively

conditions

$$\begin{aligned} u_1 &= 10^{-3}\left(x_1 + (1/2)x_2\right) \,, \\ u_2 &= 10^{-3}\left(x_1 + x_2\right) \,, \\ \omega &= \left(1/4 + 1/(4\alpha)\right) 10^{-3} \,, \\ f_1 &= f_2 = 0 \,, \\ m &= 1 \,, \end{aligned} \tag{14}$$

where the parameter $\alpha$ is $1 - k$. The relative analytical solution in terms of stresses are:

$$\begin{aligned} \sigma_{11} &= \sigma_{22} = 4 \,, \\ \sigma_{12} &= 1 \,, \\ \sigma_{21} &= 2 \,, \\ \mu_1 &= \mu_2 = 0 \,. \end{aligned} \tag{15}$$

The solution obtained are shown in Figs. 5 and 6.

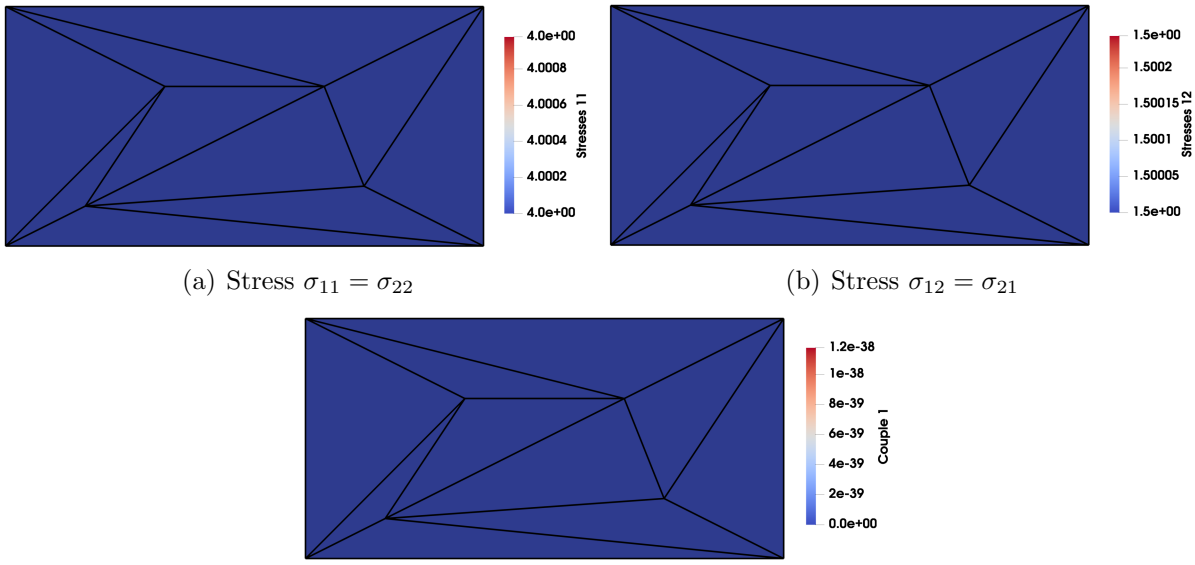


(a) Stress $\sigma_{11} = \sigma_{22}$

(b) Stress $\sigma_{12} = \sigma_{21}$

(c) Couple $\mu_1 = \mu_2$

**Figure 3**: Stress solution for path test 1 with triangular mesh

### 3.3 Patch Test 3

The *patch test 3* tests a general case of Cosserat continuum. The following boundary conditions are imposed

$$\begin{aligned} u_1 &= 10^{-3}\,(x_1 + (1/2)x_2)\ , \\ u_2 &= 10^{-3}\,(x_1 + x_2)\ , \\ \omega &= (1/4 + 1/(2\alpha)(x_1 - x_2))\,10^{-3}\ , \\ f_1 &= f_2 = 1\ , \\ m &= 2(x_1 - x_2)\ , \end{aligned} \tag{16}$$

and the relative solution:

$$\begin{aligned} \sigma_{11} &= \sigma_{22} = 4\ , \\ \sigma_{12} &= 1.5 - (x_1 - x_2)\ , \\ \sigma_{21} &= 1.5 + (x_1 - x_2)\ , \\ \mu_1 &= -\mu_2 = (2l^2/\alpha)\ . \end{aligned} \tag{17}$$

The contour plot of the stresses for triangular and Voronoi meshes are shown in Fig. 7 and Fig. 8 respectively. In Tab. 2 the displacements and the stresses at the point P (see Fig. 1(a)) are reported and compared with the exact solution. All results in the Tab. 2 are refereed to the triangular mesh. The Virtual Element (VEM), here proposed, shows improved performances compared with the MLINT (linear displacement and rotation), MQLT (quadratic displacement and linear rotation) and MQUAT (quadratic displacement and rotation) elements proposed by [24].

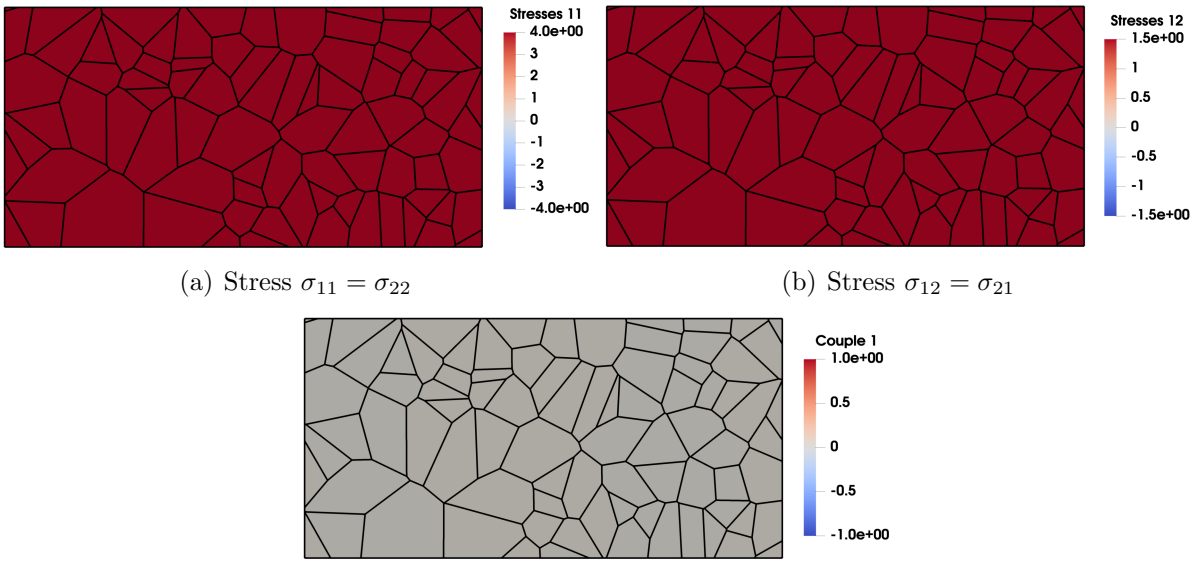


(a) Stress $\sigma_{11} = \sigma_{22}$

(b) Stress $\sigma_{12} = \sigma_{21}$

(c) Couple $\mu_1 = \mu_2$

**Figure 4**: Stress solution for path test 1 with Voronoi mesh

**Table 2**: Patch test 3: displacements at node 2 and stresses at $P = (0.0933, 0.06)$ using triangular mesh

| | $u_1 \times 10^3$ | $u_2 \times 10^3$ | $\omega \times 10^3$ | $\sigma_{11}$ | $\sigma_{12}$ | $\mu_1$ |
|---|---|---|---|---|---|---|
| MLINT | 0.1944 | 0.2096 | 0.4001 | 3.9928 | 1.4634 | 0.0400 |
| MQLT | 0.1945 | 0.2097 | 0.4001 | 3.9956 | 1.4668 | 0.0400 |
| MQUAT | 0.1945 | 0.2097 | 0.3960 | 3.9956 | 1.4707 | 0.0392 |
| VEM | 0.1950 | 0.2100 | 0.3998 | 4.0000 | 1.4668 | 0.0399 |
| *Exact* | 0.1950 | 0.2100 | 0.4000 | 4.0000 | 1.4667 | 0.0400 |

## 4 FINAL REMARKS

In the present work we developed a novel formulation of the Virtual Element methodology for 2D micropolar linear elastic continuum. In particular we adopt linear Virtual Element Method both for displacements and rotations. The formulation developed and implemented is in good agreement with the patch tests presented in literature and all tests are passed for the standard triangular mesh and for distorted Voronoi mesh.

### Acknowledgment

This research was supported by Italian Ministry of University and Research: PRIN 2015, project 2015JW9NJT (B86J16002300001); Sapienza Research Grants 'Grandi Progetti' 2016 (B82F16005920005) and 'Progetti Medi' 2017 (B83C17001440005).

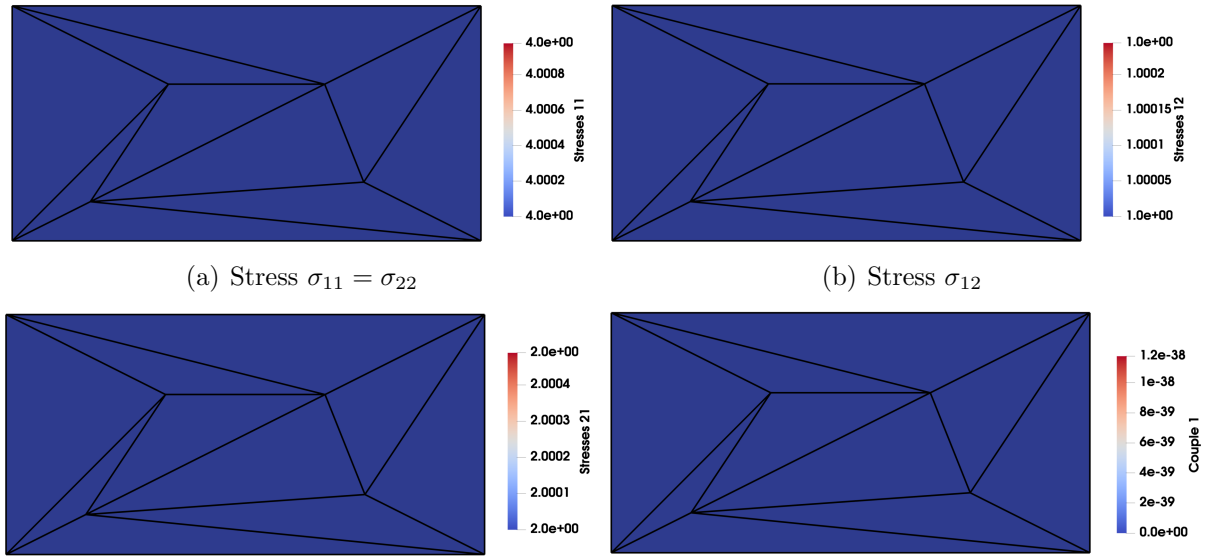


(a) Stress $\sigma_{11} = \sigma_{22}$ (b) Stress $\sigma_{12}$

(c) Stress $\sigma_{21}$ (d) Couple $\mu_1 = \mu_2$

**Figure 5**: Stress solution for path test 2 with triangular mesh

## REFERENCES

[1] D. Addessi, M. De Bellis, and E. Sacco. Micromechanical analysis of heterogeneous materials subjected to overall Cosserat strains. *Mechanics Research Communications*, 54:27–34, 2013.

[2] E. Artioli, L. Beiro da Veiga, C. Lovadina, and E. Sacco. Arbitrary order 2D virtual elements for polygonal meshes: part II, inelastic problem. *Computational Mechanics*, 60(4):643–657, 2017.

[3] E. Artioli, S. Marfia, and E. Sacco. High-order virtual element method for the homogenization of long fiber nonlinear composites. *Computer Methods in Applied Mechanics and Engineering*, 341:571–585, 2018.

[4] A. Ask, S. Forest, B. Appolaire, and K. Ammar. A Cosseratphase-field theory of crystal plasticity and grain boundary migration at finite deformation. *Continuum Mechanics and Thermodynamics*, 2018. Article in Press, DOI: 10.1007/s00161-018-0727-6.

[5] L. Beiro Da Veiga, F. Brezzi, A. Cangiani, G. Manzini, L. Marini, and A. Russo. Basic principles of virtual element methods. *Mathematical Models and Methods in Applied Sciences*, 23(1):199–214, 2013.

[6] L. Beiro Da Veiga, F. Brezzi, and L. Marini. Virtual elements for linear elasticity problems. *SIAM Journal on Numerical Analysis*, 51(2):794–812, 2013.

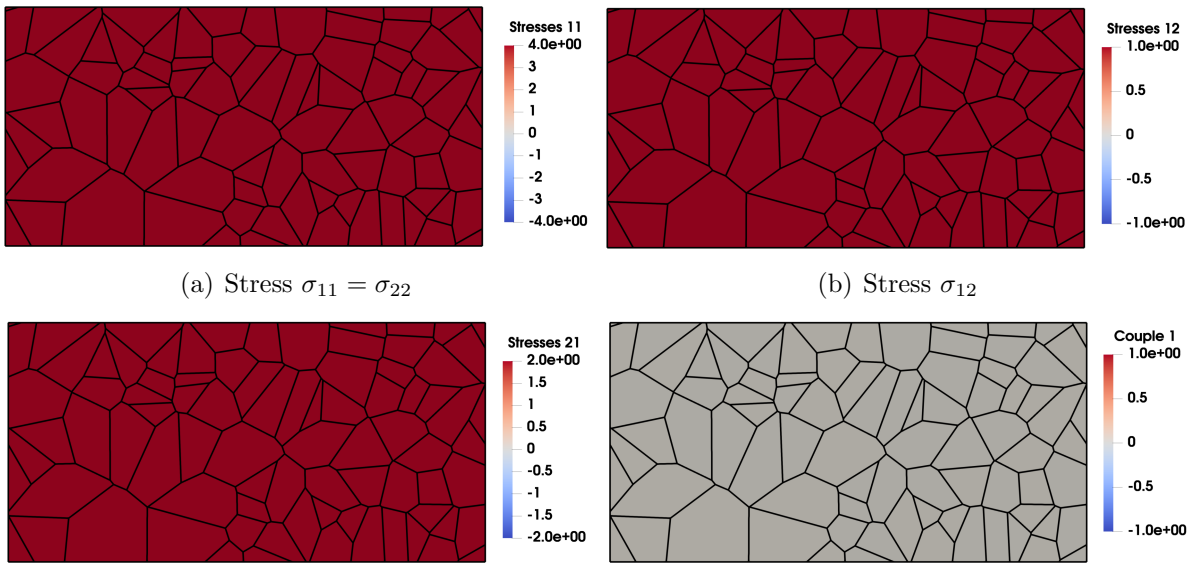


(a) Stress $\sigma_{11} = \sigma_{22}$ (b) Stress $\sigma_{12}$

(c) Stress $\sigma_{21}$ (d) Couple $\mu_1 = \mu_2$

**Figure 6**: Stress solution for path test 2 with Voronoi mesh

[7] L. Beiro Da Veiga, F. Brezzi, L. Marini, and A. Russo. Mixed virtual element methods for general second order elliptic problems on polygonal meshes. *ESAIM: Mathematical Modelling and Numerical Analysis*, 50(3):727–747, 2016.

[8] H. Chi, L. Beiro da Veiga, and G. Paulino. A simple and effective gradient recovery scheme and a posteriori error estimator for the Virtual Element Method (VEM). *Computer Methods in Applied Mechanics and Engineering*, 347:21–58, 2019.

[9] L. Da Veiga, F. Brezzi, L. Marini, A. Russo, F. Brezzi, and G. Manzini. The Hitchhiker's guide to the virtual element method. *Mathematical Models and Methods in Applied Sciences*, 24(8):1541–1573, 2014.

[10] M. De Bellis, P. Wriggers, B. Hudobivnik, and G. Zavarise. Virtual element formulation for isotropic damage. *Finite Elements in Analysis and Design*, 144:38–48, 2018.

[11] A. Eringen. *Microcontinuum field theories*. Springer-Verlag, New York, 1999.

[12] N. Fantuzzi, L. Leonetti, P. Trovalusci, and F. Tornabene. Some Novel Numerical Applications of Cosserat Continua. *International Journal of Computational Methods*, 15(6), 2018.

[13] J. Fatemi, P. Onck, G. Poort, and F. Van Keulen. Cosserat moduli of anisotropic cancellous bone: A micromechanical analysis. volume 105, pages 273–280, 2003.

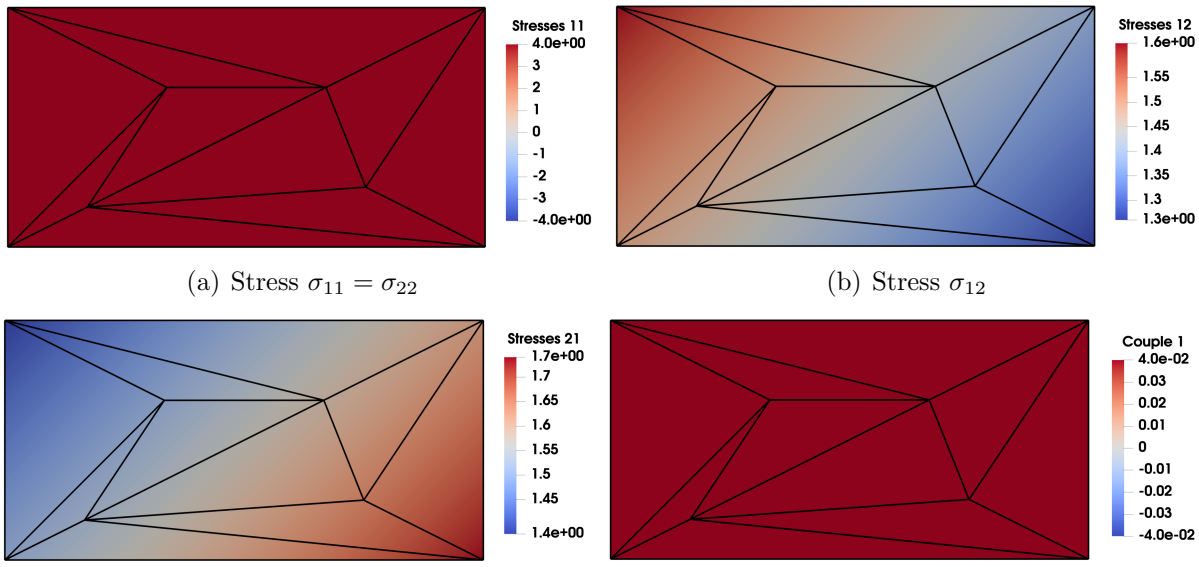


(a) Stress $\sigma_{11} = \sigma_{22}$ (b) Stress $\sigma_{12}$

(c) Stress $\sigma_{21}$ (d) Couple $\mu_1 = -\mu_2$

**Figure 7**: Stress solution for path test 3 with triangular mesh

[14] B. Hudobivnik, F. Aldakheel, and P. Wriggers. A low order 3d virtual element formulation for finite elastoplastic deformations. *Computational Mechanics*, 63(2):253–269, 2019.

[15] G. Htter. On the micro-macro relation for the microdeformation in the homogenization towards micromorphic and micropolar continua. *Journal of the Mechanics and Physics of Solids*, 127:62–79, 2019.

[16] G. Htter, U. Mhlich, and M. Kuna. Micromorphic homogenization of a porous medium: elastic behavior and quasi-brittle damage. *Continuum Mechanics and Thermodynamics*, 27(6):1059–1072, 2015.

[17] R. Lakes. Experimental microelasticity of two porous solids. *International Journal of Solids and Structures*, 22(1):55–63, 1986.

[18] R. Lakes. Elastic and viscoelastic behavior of chiral materials. *International Journal of Mechanical Sciences*, 43(7):1579–1589, 2001.

[19] L. Leonetti, N. Fantuzzi, P. Trovalusci, and F. Tornabene. Scale effects in orthotropic composite assemblies as micropolar continua: A comparison between weak and strong-form finite element solutions. *Materials*, 12(5), 2019.

[20] V. Nguyen-Thanh, X. Zhuang, H. Nguyen-Xuan, T. Rabczuk, and P. Wriggers. A Virtual Element Method for 2d linear elastic fracture analysis. *Computer Methods in Applied Mechanics and Engineering*, 340:366–395, 2018.

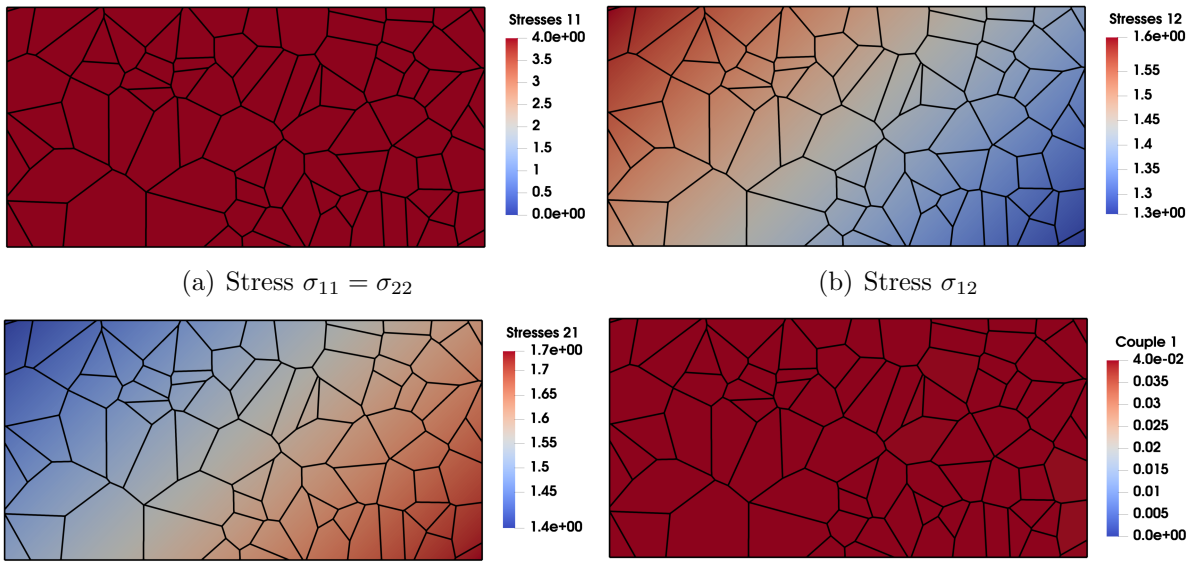


(a) Stress $\sigma_{11} = \sigma_{22}$

(b) Stress $\sigma_{12}$

(c) Stress $\sigma_{21}$

(d) Couple $\mu_1 = -\mu_2$

**Figure 8**: Stress solution for path test 3 with Voronoi mesh

[21] P. Onck. Cosserat modeling of cellular solids. *Comptes Rendus - Mecanique*, 330(11):717–722, 2002.

[22] M. Pingaro, E. Reccia, and P. Trovalusci. Homogenization of random porous materials with low order Virtual Elements. *ASCE-ASME Journal of Risk and Uncertainty in Engineering Systems Part B: Mechanical Engineering*, 2019. Article in Press, DOI: 10.1115/1.4043475.

[23] M. Pingaro, E. Reccia, P. Trovalusci, and R. Masiani. Fast statistical homogenization procedure (FSHP) for particle random composites using virtual element method. *Computational Mechanics*, 2019. Article in Press, DOI: 10.1007/s00466-018-1665-7.

[24] E. Providas and M. Kattis. Finite element method in plane Cosserat elasticity. *Computers and Structures*, 80(27-30):2059–2069, 2002.

[25] B. Reddy and D. van Huyssteen. A virtual element method for transversely isotropic elasticity. *Computational Mechanics*, 2019. Article in Press, DOI: 10.1007/s00466-019-01690-7.

[26] Z. Rueger, C. Ha, and R. Lakes. Cosserat elastic lattices. *Meccanica*, 2019.

[27] Z. Rueger and R. Lakes. Experimental Cosserat elasticity in open-cell polymer foam. *Philosophical Magazine*, 96(2):93–111, 2016.

[28] Z. Rueger and R. Lakes. Strong Cosserat Elasticity in a Transversely Isotropic Polymer Lattice. *Physical Review Letters*, 120(6), 2018.

[29] V. Sansalone, P. Trovalusci, and F. Cleri. Multiscale modeling of materials by a multifield approach: Microscopic stress and strain distribution in fiber-matrix composites. *Acta Materialia*, 54(13):3485–3492, 2006.

[30] V. Settimi, P. Trovalusci, and G. Rega. Dynamical properties of a composite microcracked bar based on a generalized continuum formulation. *Continuum Mechanics and Thermodynamics*, 2019. Article in Press, DOI: 10.1007/s00161-019-00761-7.

[31] I. Stefanou, J. Sulem, and I. Vardoulakis. Three-dimensional Cosserat homogenization of masonry structures: Elasticity. *Acta Geotechnica*, 3(1):71–83, 2008.

[32] P. Trovalusci. Molecular Approaches for Multifield Continua: origins and current developments. *CISM International Centre for Mechanical Sciences, Courses and Lectures*, 556:211–278, 2014. Springer, Vienna.

[33] P. Trovalusci, M. De Bellis, M. Ostoja-Starzewski, and A. Murrali. Particulate random composites homogenized as micropolar materials. *Meccanica*, 49(11):2719–2727, 2014.

[34] P. Trovalusci and R. Masiani. Non-linear micropolar and classical continua for anisotropic discontinous materials. *International Journal of Solids and Structures*, 40(5):1281–1297, 2003.

[35] P. Trovalusci, M. Ostoja-Starzewski, M. De Bellis, and A. Murrali. Scale-dependent homogenization of random composites as micropolar continua. *European Journal of Mechanics, A/Solids*, 49:396–407, 2015.

[36] P. Trovalusci and A. Pau. Derivation of microstructured continua from lattice systems via principle of virtual works: The case of masonry-like materials as micropolar, second gradient and classical continua. *Acta Mechanica*, 225(1):157–177, 2014.

[37] P. Trovalusci, V. Varano, and G. Rega. A generalized continuum formulation for composite microcracked materials and wave propagation in a bar. *Journal of Applied Mechanics*, 77(6), 2010.

[38] O. Zienkiewicz and R. Taylor. *Finite Element Method: Volume 1 - The Basis*. Butterworth-Heinemann, Oxford, 5th edition, 2000.